Title

Antimitochondrial Antibody Recognition and Structural Integrity of the Inner Lipoyl Domain of the E2 Subunit of Pyruvate Dehydrogenase Complex

Journal

The Journal of Immunology, 191(5)

ISSN

0022-1767

Authors

Wang, Jinjun
Budamagunta, Madhu S
Voss, John C
et al.

Publication Date

2013-09-01

DOI

10.4049/jimmunol.1301092

Peer reviewed

Published in final edited form as:
J Immunol. 2013 September 1; 191(5): 2126–2133. doi:10.4049/jimmunol.1301092.

AMA recognition and structural integrity of the inner lipoyl domain of the E2 subunit of pyruvate dehydrogenase complex (PDC-E2)[1]

Jinjun Wang[*], **Madhu S. Budamagunta**[†], **John C. Voss**[†], **Mark J. Kurth**[‡], **Kit S. Lam**[§], **Ling Lu**[¶], **Thomas P. Kenny**[*], **Christopher Bowlus**[‖], **Kentaro Kikuchi**[#], **Ross L. Coppel**[**], **Aftab A. Ansari**[††], **M. Eric Gershwin**[*], and **Patrick S.C. Leung**[*]

[*]Division of Rheumatology/Allergy and Clinical Immunology, University of California, Davis, CA 95616, USA

[†]Biochemistry and Molecular Medicine, School of Medicine, University of California, Davis, California 95616, USA

[‡]Department of Chemistry, University of California, Davis, CA 95616, USA

[§]Department of Biochemistry and Molecular Medicine, University of California, Davis, California 95817, USA

[¶]College of Life Sciences, Nanjing Normal University, Nanjing, China

[‖]Division of Gastroenterology and Hepatology, University of California Davis Medical Center, Sacramento, USA

[#]The Fourth Department of Internal Medicine, Teikyo University, Kanagawa, Japan

[**]Department of Microbiology, Monash University, Clayton, Victoria, Australia

[††]Department of Pathology, Emory University School of Medicine, Atlanta, GA 30322

Abstract

Antimitochondrial autoantibodies (AMA), the serological hallmark of primary biliary cirrhosis (PBC) are directed against the lipoyl domain of the E2 subunit of pyruvate dehydrogenase (PDC-E2). However, comprehensive analysis of the amino acid residues of PDC-E2 lipoyl beta sheet with AMA specificity is lacking. Herein, we postulated that specific residues within the lipoyl domain are critical to AMA recognition by maintaining conformational integrity. We systematically replaced each of 19 residue peptides of the inner lipoyl domain with alanine and analyzed these mutants for reactivities against 60 PBC and 103 control sera. Based on these data, we then constructed mutants with 2, 3, or 4 replacements and, in addition, probed the structure of the substituted domains using thiol-specific spin labeling and electron paramagnetic resonance (EPR) of a ^{5}Ile-> Ala and ^{12}Ile->Ala double mutant. Single alanine replacement at ^{5}Ile, ^{12}Ile and ^{15}Glu significantly reduced AMA recognition. In addition, mutants with 2, 3, or 4 replacements at ^{5}Ile, ^{12}Ile and ^{15}Glu reduced AMA reactivity even further. Indeed, EPR reveals a highly flexible structure within the ^{5}Ile and ^{12}Ile double-alanine mutant. Autoreactivity is largely focused on specific residues in the PDC-E2 lipoyl domain critical in maintaining the lipoyl loop

[1]**Grant Support**: This work is supported in part by National Institutes of Health grants DK39588 and DK067003

Correspondence: M. Eric Gershwin, M.D. Division of Rheumatology, Allergy and Clinical Immunology, University of California School of Medicine, 451 Health Sciences Drive, Suite 6510, Davis, CA 95616; megershwin@ucdavis.edu; Phone: 530-752-2884; Fax: 530-752-4669. OR Patrick S.C. Leung, Ph.D., Division of Rheumatology, Allergy and Clinical Immunology, University of California School of Medicine, 451 Health Sciences Drive, Suite 6510, Davis, CA 95616; psleung@ucdavis.edu; Phone: 530-754-4943; Fax: 530-754-6047.

conformation necessary for AMA recognition. Collectively, the AMA binding studies and EPR analysis demonstrate the necessity of the lipoyl beta sheet structural conformation in anti-PDC-E2 recognition.

Keywords

Autoantibodies; primary biliary cirrhosis; xenobiotics; conformational structure

Introduction

The autoantigens recognized by antimitochondrial autoantibodies (AMA) are identified as the E2 subunits of the 2-oxo-acid dehydrogenase mitochondrial enzyme complex (2-OADC E2) particularly, the E2 subunits of pyruvate dehydrogenase (PDC-E2) (1–6). Interestingly, the AMA epitopes of these autoantigens are mapped within the lipoic acid binding domain (7). Accumulating evidence implicates that the loss of tolerance to the 2-OADC E2 subunits is pivotal in the initiation event of PBC and that AMA specificities reflect aspects to the induction phase of the disease (7, 8). Recent data further suggest that chemical modification of the PDC-E2 lipoic acid, via an electrophilic attack on the lipoic acid disulfide bond, triggers the breakage of tolerance to PDC-E2 (9, 10). Such modifications could substantially affect the conformation of the PDC-E2 lipoyl domain and its immunogenicity in genetically susceptible hosts.

High-resolution structural analysis and modeling studies of the PDC-E2 lipoyl domains from both prokaryotes and eukaryotes demonstrated that lipoic acid is covalently attached to the ε group of lysine (K) via an amide bond and is prominently displayed on the outer surface of PDC-E2 (11). More importantly, the ability of lipoic acid to rotate by means of a “swinging arm”, with respect to the bulk of the PDC-E2 molecule, allows access to its dithionate ring for reduction and acylation (9, 12). Although the change in conformation and the existence of multiple conformations of the lipoyl domain during reductive acetylation is important in catalyzing acyl transfer, it also renders PDC-E2 susceptible to aberrant chemical modification (13). Such chemical modification of PDC-E2 would generate neo-antigens. We hypothesize that in PDC-E2, a fully formed β-sheet at the lipoylated region, will elicit the highest AMA specificity. In this study we define the residues in the PDC-E2 lipoyl domain that are indispensable in AMA recognition. We have performed alanine mutagenesis scanning in which each residue is replaced along a 19 residue stretch of the PDC-E2 lipoyl domain with alanine. Recombinant proteins of each of these mutants were studied for their serological reactivity against a panel of serum samples from patients with PBC and controls. In addition, four mutants with double residue substitutions, two mutants with triple residue substitutions, and one mutant with quadruple residue substitution were studied. The structural effects of substitutions in a mutant with double residue substitutions and its interaction with AMA were also studied by electron paramagnetic resonance. Our data demonstrate that specific amino acid residues within the PDC-E2 lipoyl domain are critical in anti-PDC-E2 recognition by maintaining the conformational integrity of the lipoyl beta sheet.

Materials and Methods

Serum samples

Serum samples from 60 AMA positive patients with histological liver lesions of PBC (staged sera: 20 stage I, 20 stage II, 20 stage III and IV), 28 patients with primary sclerosing cholangitis (PSC), 30 patients with systemic lupus erythematosus (SLE), 20 patients with Crohn’s disease, 20 patients with scleroderma and 5 healthy controls were obtained

following informed consent and used for these studies. The clinical diagnosis was verified using published criteria (14–17). The protocol was approved by the Institutional Review Board of the University of California at Davis.

Site-directed mutagenesis of the PDC-E2 lipoyl domain

Using the QuickChange II Site-directed Mutagenesis kit (Agilent Technologies, Santa Clara, CA), residues within a 19 residue stretch (LLAEIETDKATIGFEVQEE) of the lipoyl domain of PDC-E2 were individually substituted by alanine to generate 17 single residue substitution mutants. Briefly, QuickChange primers were designed with the QuickChange Primer Design Program (Agilent-Stratagene; http://www.stratagene.com). The basic procedure utilizes a supercoiled plasmid of pGEX vector expression clone containing a 413 bp insert encoding the human PDC-E2 domain and two synthetic oligonucleotide primers, both containing the desired mutation. The oligonucleotide primers, each complementary to opposite strands of the vector, are extended during temperature cycling by PfuUltra HF DNA polymerase (Agilent-Stratagene, La Jolla, CA), without primer displacement (Initial denaturation at 94°C for 20 sec, followed by 18 cycles of denaturation at 95°C for 30 sec, annealing at 55°C for 1 min and extension at 68°C for 5 min, and final extension at 68°C for 10 min). Extension of the oligonucleotide primers generates a mutated plasmid containing staggered nicks. Following temperature cycling, the product is treated with Dpn I. The Dpn I endonuclease (target sequence: 5´-Gm6ATC-3´) is specific for methylated and hemimethylated DNA and is used to digest the parental DNA template and to select for mutation-containing synthesized DNA. The nicked vector DNA containing the desired mutations was then transformed into *E. coli* XL1-Blue supercompetent cells (Agilent-Stratagene, La Jolla, CA). Plasmid DNA from each mutant construct was purified for nucleotide sequence determination using the ABI 3730 DNA sequencers (Davis Sequencing, Davis, CA). Thereafter, 4 mutants with double residue substitutions (with recombinant proteins of alanine replacement at the position 5, 12; 2, 12; 2, 15; and 5, 15), 2 mutants with triple residue substitutions (with recombinant proteins of alanine replacement at the position 2, 5, 12 and 5, 12, 15), and 1 mutant with quadruple residue substitution (with recombinant proteins of alanine replacement at the position 2, 5, 12, 15) were constructed similarly (Figure 1 & Table I).

Preparation of mutant rPDC-E2 proteins

rPDC-E2 protein was prepared as described (18) and protein concentrations determined by bicinchoninic acid (BCA) assay (Thermo Scientific). The specificity of the purified recombinant proteins was verified by immunoblotting with 2H4, an anti-PDC-E2 monoclonal antibody (19). Positive and negative controls were included throughout. We removed the GST tag as previously described (13).

Purification of IgG

Human serum samples (10 PBC, 5 healthy controls) were individually adjusted to the composition of the binding buffer (20 mM sodium phosphate, pH 7.0) by diluting the sample with binding buffer. Sera samples were first centrifuged before loading on the HiTrap Protein G column (GE Healthcare, Piscataway, NJ). The column was washed with 10 column volumes of binding buffer at 1 ml/min, then the samples were applied. Thereafter, the columns were washed with 5–10 column volumes of binding buffer and eluted with 10 column volumes of elution buffer (0.1 M glycine-HCl, pH 2.7), and immediately neutralized by adding 200 μl 1 M Tris-HCl, pH 9.0.

Determination of anti-PDCE2 reactivity

96-well ELISA plates were coated with either recombinant proteins of PDC-E2 or PDC-E2 mutants (10 microgram/mL) in carbonate coating buffer, pH 9.6 at 4°C overnight, blocked with 3% non-fat dry milk, and then incubated with diluted serum (1:4000 for PBC sera and 1:1000 in non-PBC controls) samples for 1 hour. Reactivity was determined as described with known positive and negative controls (13). Intra assay variability was determined with multiple dilutions (1:4,000, 1:8000, 1:16,000 and 1:32,000) of a PBC serum sample with 5 repeats of each dilution.

Electron paramagnetic resonance (EPR)

Electron paramagnetic resonance was used to probe the structure of the alanine-substituted inner lipoyl domain (20–25). In brief, spins labeled mutants were produced by substituting a cysteine residue at specific sites within the human PDC-E2 lipoyl region using mutagenic oligonucleotides and iProof polymerase (Bio-Rad, Hercules, CA). Double mutants 3 and 4 were chosen for EPR because the AMA reactivity decreases dramatically when compared with wild type. Unless otherwise indicated, attachment of the nitroxide spin label to the cysteine was achieved by treating the purified protein with 500 μM (1-oxyl-2,2,5,5-tetramethyl-3-pyrroline-3-methyl) methanethiosulfonate (MTSL; Toronto Research Chemicals, Toronto, Canada). Following a 30 min incubation time, the sample was passed over a Biospin 6 (BioRad) size exclusion column to unincorporated label. Labeled samples were concentrated using a 10 kDa MWCO Amicon Ultra centrifugal filter device (Millipore Corp., Billerica, MA) to a concentration of ~ 1mg/ml. For EPR measurement, 5 μl of concentrated sample was combined with 5 μl of either buffer or purified IgG and incubated for 30 min at room temperature. An aliquot (~5 μl) was then loaded into a sealed quartz capillary and measured in a JEOL X-band EPR spectrometer fitted with a loop-gap resonator. Spectra were acquired at room temperature (20–22 °C) from a single 60-s scan over a field of 100 G at a microwave power of 2 mW and a modulation amplitude optimized to the natural line width of the individual spectrum (0.5 – 1.5 G).

Statistical analysis

A two-tailed unpaired t-test with Welch's correction was used to analyze the Ig reactivity against PDC-E2 mutant proteins. Statistical significance was determined by a two-tailed unpaired t-test with Welch's correction.

Results

Construction and expression of mutant rPDC-E2 lipoyl domain

Each position within a 19 residue stretch of the lipoyl domain of PDC-E2 was individually substituted by alanine to generate 17 single residue substitutions mutants, 4 mutants with double residue substitutions, 2 mutants with triple residue substitutions, and 1 mutant with quadruple residue substitution (Table I). Plasmid DNA was purified from each individual mutant for nucleotide sequence determination to confirm the presence of the mutations. Recombinant protein from each of the constructs migrated at 42 kDa, corresponding to the GST-PDC-E2 fusion protein (Figure 1).

Immunoreactivity of rPDC E2 mutant protein to PBC sera

60/60 AMA-positive PBC sera recognized the wild type rPDC-E2 by ELISA whereas none of 103 control sera reacted to rPDC E2 wild type or mutant proteins. Alanine replacements of isoleucine at positions 5 or 12 or glutamic acid at position 15 significant reduced AMA reactivity (47.6%±2.9%,70.6%±2.9%,65.9%±3.4% respectively) compared with the wild type rPDC E2 (Table II and Figure 2). Recombinant proteins with alanine substitution at

position 5, 12 and 15 analyzed for AMA recognition by purified IgG prepared from a subgroup of 10 AMA positive sera. Mean reactivity of IgG against these mutated proteins was reduced even further than seen with whole sera (40.8% ± 5.2%, 55.2% ± 6.5%, 48.2% ± 7.4% respectively). AMA reactivity to the recombinant protein mutated at both isoleucine residues was reduced to only 6.6% ± 0. 9% of wild type reactivity (Table II), again a marked reduction in binding also seen using purified IgG. Notably, enhanced IgM AMA recognitions were observed with mutants PM7, 8, 16 and 17. Based upon the variability of AMA bindings to specific mutants, we thence addressed whether this variation was a result of mixed autoantibody population and/or differences in titers between patients, by further analysis at 4 serial dilutions and including 5 replicates for each dilution (Figure 3). We note that the low intraassay variation and the reproducibility of the AMA binding at all the serial dilutions studied support the presence of a dominant population of anti-PDC-E2 lipoyl domain reactivity. The patterns of binding seen were similar for both IgG and IgM as evidenced by binding studies which were read out with specific anti-isotype antisera (Figure 4).

Probing the mutated rPDC-E2 lipoyl domain with site-directed spin labels

To probe the structure of the alanine-substituted inner lipoyl domain, thiol-specific spin labels were attached to single cysteine replacements introduced at positions neighboring Ala5 and Ala12 in the PDM 3 mutant. The resulting Cys replacements localized the spin label to either position Glu4, Gly13, or both positions in the double Cys mutant. Each of the three variations of PDM 3 were purified, reacted with MTSL spin label, and analyzed by EPR spectroscopy. As shown in Figure 4, spin labels at positions 4 and 13 of the lipoyl domain display a similar weakly immobilized spectrum, indicating a relatively disordered loop structure in the presence of the double-Ala mutation. The effect of adding a stoichiometric amount of IgG isolated from PBC sera was also examined and compared to the effects of IgG from healthy controls. Due to the large size of Ig, it is expected that the high affinity binding of the PBC antibody would dramatically decrease the local and global rotation diffusion of the attached spin labels, producing a much more broadened EPR spectrum. However, only moderate broadening is observed at either position 4 or 13 upon addition of PBC antibody, with the effect slightly higher at position 13. Control IgG produces no significant effect. The moderate effects of PBC IgG on spin label dynamics is consistent with the drastically reduced antibody binding to the PDM 3 mutant.

Previous studies suggested that the inner lipoyl domain assumes the loop structure shown in Figure 1B. In this prediction, positions Glu4 and Gly13 should be approximately opposite one another. To test whether this proximity is maintained in the PDM3 mutant, we searched for evidence of dipolar coupling between nitroxide spin labels placed at positions 4 and 13 of the PDC-E2 lipoyl domain. Significant dipolar coupling can be detected when spin labels are within 2 nm of each other, resulting in spectral broadening (26). Thus, a double-Cys replacement mutant was made to place spin labels at positions 4 and 13, and the MTSL-labeled protein examined by EPR. The resulting spectrum (Figure 4) is severely broadened, indicative of strong dipolar coupling. This result demonstrates that the close (1–1.5 nm) proximity of these positions is maintained in the context of the Ala5/Ala12 mutant. As expected from the low PBC binding to this mutant, addition of this antibody to the double spin-labeled protein does not significantly alter the composite spectrum (Figure 5).

Discussion

In light of the unique epitope specificity of AMA and the conformational significance of the PDC-E2 lipoyl loop beta sheet structure at the surface of PDC-E2 in relation to its biochemical function in acyl transfer during oxidative phosphorylation, we set out to define the critical residue residues responsible for AMA recognition. Firstly, we have chosen a 19

residue sequence that encompasses the entire beta sheet structure of the PDC-E2 lipoyl domain and systematically replaced each residue along this 19 residue stretch with alanine. These mutants were constructed using a well-characterized expression clone of PDC-E2 inner lipoyl domain in pGEX 4T-1 that encompasses the auto epitope (27). Subsequently, these PDC-E2 lipoyl domain residue substitution mutants were individually analyzed for their reactivity with 60 AMA positive sera from patients with PBC. Our data reflect that total serum IgG binding to three of the mutants were significantly reduced and total serum IgM reactivity to one of the mutants was significantly reduced when compared to the wild type. The mutants had mutations at isoleucine at positions 5 and 12 and glutamic acid at position 15 of the 19-residue lipoyl beta sheet. Interestingly, when purified IgG was examined for its binding reactivity to the mutants, mutations in residue position number 5 and mutations along the stretch of residues 12 to 15 also significantly reduced IgG binding. Structurally, the isoleucine residues (positions 5 and 12) are directly opposite each other in the lipoyl beta sheet and residues 13–15 (glycine, phenylalanine, glutamic acid) are the nearest neighbors to the isoleucine residue at position 12. The interactions of the hydrophobic arm of isoleucine residues 5 and 12 and these neighboring residues are important in maintaining the beta sheet conformation of this structure.

We next addressed whether these mutations, if combined in the same sequence, would exhibit any additional decrease in AMA binding. Hence, we designed double, triple and quadruple mutants and have focused on the two isoleucine residues at position 5 and 12. Our data demonstrate that alanine substitution mutants at both isoleucine residues markedly decreased IgG and IgM AMA recognition when compared to the single residue substitutions or single isoleucine substitutions with residue substitutions at another position (Table II). Our data from MTSL spin labeling and EPR spectroscopy of Cys substitutions positions at Glu 4 and Gly13 of the lipoyl domain of the Ala substitution mutant PDM3 verifies the importance of the isoleucine residues at position 5 and 12 in maintaining the integrity of the loop structure of the PDC-E2 inner lipoyl domain (Figure 4). This data, together with the antibody binding data of the single mutants PM4, PM 10 and double mutants PD3with PBC sera further reaffirm the necessity of the lipoyl loop structure in anti-PDCE2 recognition. Interestingly, several alanine substitutions within the PDC-E2 inner lipoyl loop resulted in higher IgM AMA recognition (PM7 from Asp to Ala, PM8 from Lys to Ala and PM 16, PM 17 from Glu to Ala.) The specific position of these amino acid residue changes, together with the change from charged side chain to non-polar amino acids in the mutants, potentially generates a more hydrophobic pocket for IgM binding enhancement. To our knowledge, this is the first comprehensive analysis of the amino acid residues within the inner lipoyl domain with regard to AMA recognition.

Interestingly, comparison of the sequence around the lipoyl lysine residue of PDC-E2 among bacterial species demonstrate that the isoleucine residue at position 12 is highly variable in bacterial species in which PDC-E2 is recognized by cross-reactive AMA (Table III). The observed cross-reactivity between the human PDC-E2 and its microbial homologue in *E. coli, N. aromaticivorans* and *Chlamydia pneumoniae*, suggests that PBC could be induced by exposure to bacterial antigens and perhaps by molecular mimicry between the human and microbial PDC-E2 (28–33). The observed serological cross-reactivity is likely secondary to other residues, based upon data of the significantly higher antibody titer to mammalian than their bacterial E2 homologues (34–37). The key differences in the anchoring residues in the lipoyl beta sheet in PBC AMA recognition together with minor differences in the protein fold are consistent with the differences in affinity of AMA between the human and microbial PDC-E2.

A distinctive serological feature of PBC is elevated IgM and high titer IgM AMA (38, 39). B cells and IgM-positive plasma cells as well as macrophages are present around

granulomas in livers of patients with PBC (40). However, detailed comparison of the epitope specificity of IgM and IgG AMA at the molecular level is lacking. Our data demonstrate that the profile of recognition of this panel of PDC-E2 mutants are highly similar indicating that the epitopes recognized by IgG and IgM AMA are highly conserved. Moreover, our data reflect that the crucial anchoring residues of the human PDC-E2 lipoyl beta sheet for IgM and IgG AMA recognition are identical amongst early and late stage PBC.

List of Abbreviations

2-OADC E2	E2 subunit of 2-oxoacid dehydrogenase complex
AMA	Antimitochondrial antibodies
BCA	bicinchoninic acid assay
BCOADC-E2	E2 subunit of branched chain 2-oxo-acid dehydrogenase
ELISA	Enzyme linked immunosorbent assay
EPR	Electron Paramagnetic Resonance
GST	glutathione s-transferase
HRP	horse-radish peroxidase
MTSL	(1-oxyl-2,2,5,5-tetramethyl-3-pyrroline-3-methyl) methanethiosulfonate
PBC	Primary biliary cirrhosis
PBS	Phosphate buffered saline
PDC-E2	E2 subunit of pyruvate dehydrogenase
PSC	Primary sclerosing cholangitis
QSAR	quantitative structure activity relationship
rPDC-E2	recombinant protein of PDC-E2
SLE	Systemic lupus erythematosus
WT	wild type

References

1. Gershwin ME, Mackay IR. The causes of primary biliary cirrhosis: Convenient and inconvenient truths. Hepatology. 2008; 47:737–745. [PubMed: 18098322]
2. Gershwin ME, Mackay IR, Sturgess A, Coppel RL. Identification and specificity of a cDNA encoding the 70 kd mitochondrial antigen recognized in primary biliary cirrhosis. Journal of immunology. 1987; 138:3525–3531.
3. Leung PS, Chuang DT, Wynn RM, Cha S, Danner DJ, Ansari A, Coppel RL, Gershwin ME. Autoantibodies to BCOADC-E2 in patients with primary biliary cirrhosis recognize a conformational epitope. Hepatology. 1995; 22:505–513. [PubMed: 7543435]
4. Moteki S, Leung PS, Dickson ER, Van Thiel DH, Galperin C, Buch T, Alarcon-Segovia D, Kershenobich D, Kawano K, Coppel RL, et al. Epitope mapping and reactivity of autoantibodies to the E2 component of 2-oxoglutarate dehydrogenase complex in primary biliary cirrhosis using recombinant 2-oxoglutarate dehydrogenase complex. Hepatology. 1996; 23:436–444. [PubMed: 8617422]
5. Oertelt S, Rieger R, Selmi C, Invernizzi P, Ansari AA, Coppel RL, Podda M, Leung PS, Gershwin ME. A sensitive bead assay for antimitochondrial antibodies: Chipping away at AMA-negative primary biliary cirrhosis. Hepatology. 2007; 45:659–665. [PubMed: 17326160]

6. Van de Water J, Gershwin ME, Leung P, Ansari A, Coppel RL. The autoepitope of the 74-kD mitochondrial autoantigen of primary biliary cirrhosis corresponds to the functional site of dihydrolipoamide acetyltransferase. The Journal of experimental medicine. 1988; 167:1791–1799. [PubMed: 2455013]
7. Hirschfield GM, Gershwin ME. The immunobiology and pathophysiology of primary biliary cirrhosis. Annual review of pathology. 2013; 8:303–330.
8. Benson GD, Kikuchi K, Miyakawa H, Tanaka A, Watnik MR, Gershwin ME. Serial analysis of antimitochondrial antibody in patients with primary biliary cirrhosis. Clinical & developmental immunology. 2004; 11:129–133. [PubMed: 15330448]
9. Leung PS, Wang J, Naiyanetr P, Kenny TP, Lam KS, Kurth MJ, Gershwin ME. Environment and primary biliary cirrhosis: Electrophilic drugs and the induction of AMA. Journal of autoimmunity. 2013
10. Leung PS, Lam K, Kurth MJ, Coppel RL, Gershwin ME. Xenobiotics and autoimmunity: does acetaminophen cause primary biliary cirrhosis? Trends in molecular medicine. 2012; 18:577–582. [PubMed: 22920894]
11. Howard MJ, Fuller C, Broadhurst RW, Perham RN, Tang JG, Quinn J, Diamond AG, Yeaman SJ. Three-dimensional structure of the major autoantigen in primary biliary cirrhosis. Gastroenterology. 1998; 115:139–146. [PubMed: 9649469]
12. Mao TK, Davis PA, Odin JA, Coppel RL, Gershwin ME. Sidechain biology and the immunogenicity of PDC-E2, the major autoantigen of primary biliary cirrhosis. Hepatology. 2004; 40:1241–1248. [PubMed: 15558739]
13. Naiyanetr P, Butler JD, Meng L, Pfeiff J, Kenny TP, Guggenheim KG, Reiger R, Lam K, Kurth MJ, Ansari AA, Coppel RL, Lopez-Hoyos M, Gershwin ME, Leung PS. Electrophile-modified lipoic derivatives of PDC-E2 elicits antimitochondrial antibody reactivity. J Autoimmun. 2011; 37:209–216. [PubMed: 21763105]
14. Kaplan MM, Gershwin ME. Primary biliary cirrhosis. N Engl J Med. 2005; 353:1261–1273. [PubMed: 16177252]
15. Bambha K, Kim WR, Talwalkar J, Torgerson H, Benson JT, Therneau TM, Loftus EV Jr, Yawn BP, Dickson ER, Melton LJ 3rd. Incidence, clinical spectrum, and outcomes of primary sclerosing cholangitis in a United States community. Gastroenterology. 2003; 125:1364–1369. [PubMed: 14598252]
16. Leung PS, Rossaro L, Davis PA, Park O, Tanaka A, Kikuchi K, Miyakawa H, Norman GL, Lee W, Gershwin ME. G. Acute Liver Failure Study. Antimitochondrial antibodies in acute liver failure: implications for primary biliary cirrhosis. Hepatology. 2007; 46:1436–1442. [PubMed: 17657817]
17. Stravitz RT, Lefkowitch JH, Fontana RJ, Gershwin ME, Leung PS, Sterling RK, Manns MP, Norman GL, Lee WM. G. Acute Liver Failure Study. Autoimmune acute liver failure: proposed clinical and histological criteria. Hepatology. 2011; 53:517–526. [PubMed: 21274872]
18. Moteki S, Leung PS, Coppel RL, Dickson ER, Kaplan MM, Munoz S, Gershwin ME. Use of a designer triple expression hybrid clone for three different lipoyl domain for the detection of antimitochondrial autoantibodies. Hepatology. 1996; 24:97–103. [PubMed: 8707289]
19. Sasaki M, Van De Water J, Kenny TP, Gallo ML, Leung PS, Nakanuma Y, Ansari AA, Coppel RL, Neuberger J, Gershwin ME. Immunoglobulin gene usage and immunohistochemical characteristics of human monoclonal antibodies to the mitochondrial autoantigens of primary biliary cirrhosis induced in the XenoMouse. Hepatology. 2001; 34:631–637. [PubMed: 11584357]
20. Hess JF, Budamagunta MS, Aziz A, FitzGerald PG, Voss JC. Electron paramagnetic resonance analysis of the vimentin tail domain reveals points of order in a largely disordered region and conformational adaptation upon filament assembly. Protein Sci. 2013; 22:47–55. [PubMed: 23109052]
21. Acar S, Carlson DB, Budamagunta MS, Yarov-Yarovoy V, Correia JJ, Ninonuevo MR, Jia W, Tao L, Leary JA, Voss JC, Evans JE, Scholey JM. The bipolar assembly domain of the mitotic motor kinesin-5. Nat Commun. 2013; 4:1343. [PubMed: 23299893]
22. Chen HK, Liu Z, Meyer-Franke A, Brodbeck J, Miranda RD, McGuire JG, Pleiss MA, Ji ZS, Balestra ME, Walker DW, Xu Q, Jeong DE, Budamagunta MS, Voss JC, Freedman SB, Weisgraber KH, Huang Y, Mahley RW. Small molecule structure correctors abolish detrimental

effects of apolipoprotein E4 in cultured neurons. J Biol Chem. 2012; 287:5253–5266. [PubMed: 22158868]

23. Aziz A, Hess JF, Budamagunta MS, Voss JC, Kuzin AP, Huang YJ, Xiao R, Montelione GT, FitzGerald PG, Hunt JF. The structure of vimentin linker 1 and rod 1B domains characterized by site-directed spin-labeling electron paramagnetic resonance (SDSL-EPR) and X-ray crystallography. J Biol Chem. 2012; 287:28349–28361. [PubMed: 22740688]
24. Nygaard EB, Lagerstedt JO, Bjerre G, Shi B, Budamagunta M, Poulsen KA, Meinild S, Rigor RR, Voss JC, Cala PM, Pedersen SF. Structural modeling and electron paramagnetic resonance spectroscopy of the human Na+/H+ exchanger isoform 1, NHE1. J Biol Chem. 2011; 286:634–648. [PubMed: 20974853]
25. Aziz A, Hess JF, Budamagunta MS, FitzGerald PG, Voss JC. Head and rod 1 interactions in vimentin: identification of contact sites, structure, and changes with phosphorylation using site-directed spin labeling and electron paramagnetic resonance. J Biol Chem. 2009; 284:7330–7338. [PubMed: 19117942]
26. Petrlova J, Hong HS, Bricarello DA, Harishchandra G, Lorigan GA, Jin LW, Voss JC. A differential association of Apolipoprotein E isoforms with the amyloid-beta oligomer in solution. Proteins. 2011; 79:402–416. [PubMed: 21069870]
27. Moteki S, Leung PSC, Dickson ER, VanThiel DH, Galperin C, Buch T, AlarconSegovia D, Kershenobich D, Kawano K, Coppel RL, Matuda S, Gershwin ME. Epitope mapping and reactivity of autoantibodies to the E2 component of 2-oxoglutarate dehydrogenase complex in primary biliary cirrhosis using recombinant 2-oxoglutarate dehydrogenase complex. Hepatology. 1996; 23:436–444. [PubMed: 8617422]
28. Bogdanos D, Pusl T, Rust C, Vergani D, Beuers U. Primary biliary cirrhosis following Lactobacillus vaccination for recurrent vaginitis. Journal of hepatology. 2008; 49:466–473. [PubMed: 18644655]
29. Bogdanos DP, Baum H, Okamoto M, Montalto P, Sharma UC, Rigopoulou EI, Vlachogiannakos J, Ma Y, Burroughs AK, Vergani D. Primary biliary cirrhosis is characterized by IgG3 antibodies cross-reactive with the major mitochondrial autoepitope and its Lactobacillus mimic. Hepatology. 2005; 42:458–465. [PubMed: 16025495]
30. Bogdanos DP, Baum H, Vergani D, Burroughs AK. The role of E. coli infection in the pathogenesis of primary biliary cirrhosis. Disease markers. 2010; 29:301–311. [PubMed: 21297249]
31. Padgett KA, Selmi C, Kenny TP, Leung PS, Balkwill DL, Ansari AA, Coppel RL, Gershwin ME. Phylogenetic and immunological definition of four lipoylated proteins from Novosphingobium aromaticivorans, implications for primary biliary cirrhosis. Journal of autoimmunity. 2005; 24:209–219. [PubMed: 15848043]
32. Leung PS, Park O, Matsumura S, Ansari AA, Coppel RL, Gershwin ME. Is there a relation between Chlamydia infection and primary biliary cirrhosis? Clin Dev Immunol. 2003; 10:227–233. [PubMed: 14768955]
33. Abdulkarim AS, Petrovic LM, Kim WR, Angulo P, Lloyd RV, Lindor KD. Primary biliary cirrhosis: an infectious disease caused by Chlamydia pneumoniae? J Hepatol. 2004; 40:380–384. [PubMed: 15123349]
34. Fussey SP, Ali ST, Guest JR, James OF, Bassendine MF, Yeaman SJ. Reactivity of primary biliary cirrhosis sera with Escherichia coli dihydrolipoamide acetyltransferase (E2p): characterization of the main immunogenic region. Proc Natl Acad Sci U S A. 1990; 87:3987–3991. [PubMed: 2187198]
35. Cha S, Leung PS, Gershwin ME, Fletcher MP, Ansari AA, Coppel RL. Combinatorial autoantibodies to dihydrolipoamide acetyltransferase, the major autoantigen of primary biliary cirrhosis. Proc Natl Acad Sci U S A. 1993; 90:2527–2531. [PubMed: 8460168]
36. Cha S, Leung PS, Coppel RL, Van de Water J, Ansari AA, Gershwin ME. Heterogeneity of combinatorial human autoantibodies against PDC-E2 and biliary epithelial cells in patients with primary biliary cirrhosis. Hepatology. 1994; 20:574–583. [PubMed: 7521314]
37. Fussey SP, Lindsay JG, Fuller C, Perham RN, Dale S, James OF, Bassendine MF, Yeaman SJ. Autoantibodies in primary biliary cirrhosis: analysis of reactivity against eukaryotic and

prokaryotic 2-oxo acid dehydrogenase complexes. Hepatology. 1991; 13:467–474. [PubMed: 1999318]

38. Duarte-Rey C, Bogdanos D, Yang CY, Roberts K, Leung PS, Anaya JM, Worman HJ, Gershwin ME. Primary biliary cirrhosis and the nuclear pore complex. Autoimmun Rev. 2012; 11:898–902. [PubMed: 22487189]
39. Moritoki Y, Lian ZX, Wulff H, Yang GX, Chuang YH, Lan RY, Ueno Y, Ansari AA, Coppel RL, Mackay IR, Gershwin ME. AMA production in primary biliary cirrhosis is promoted by the TLR9 ligand CpG and suppressed by potassium channel blockers. Hepatology. 2007; 45:314–322. [PubMed: 17256753]
40. You Z, Wang Q, Bian Z, Liu Y, Han X, Peng Y, Shen L, Chen X, Qiu D, Selmi C, Gershwin ME, Ma X. The immunopathology of liver granulomas in primary biliary cirrhosis. J Autoimmun. 2012; 39:216–221. [PubMed: 22727562]

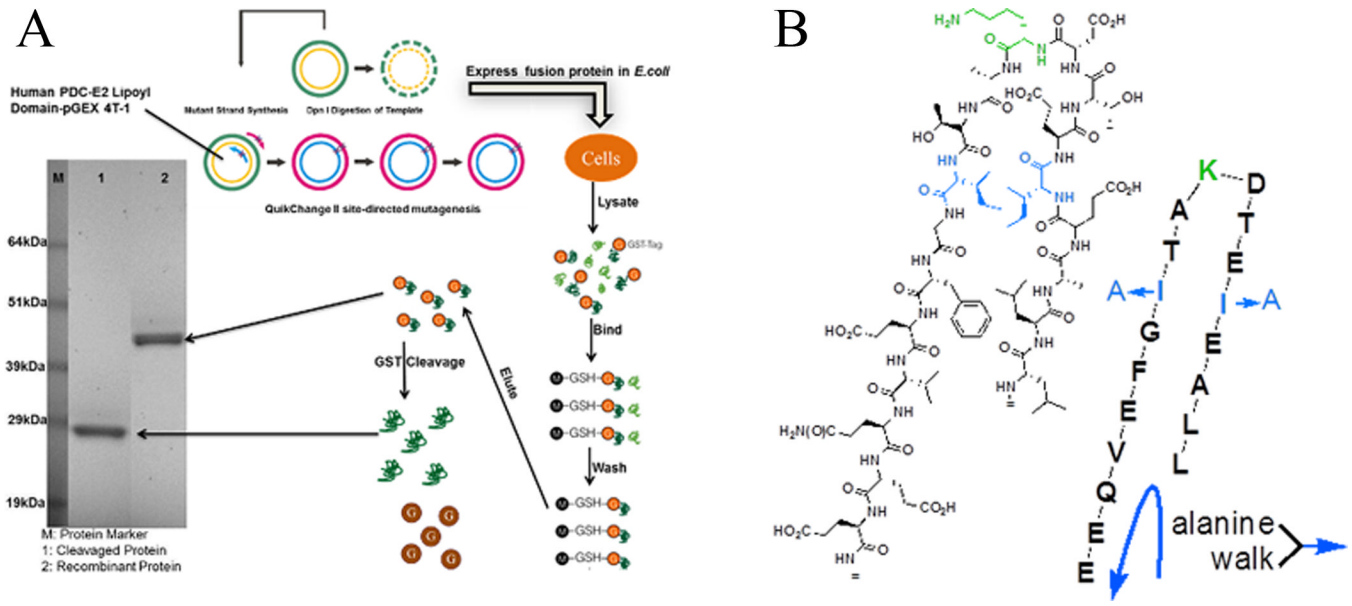

Figure 1.

A. Construction and expression of alanine substitution mutants of the human PDC-E2 lipoyl domain. Recombinant protein from PDC-E2 mutant was purified through a glutathione agarose column. Each mutant protein was confirmed by SDS-PAGE. Figure 1B. Schematic representation of the PDC-E2 lipoyl domain including the 19 residues (LLAEI-ETDKA-TIGFE-VQEE), noting the direction of the alanine walk direction is from L to E.

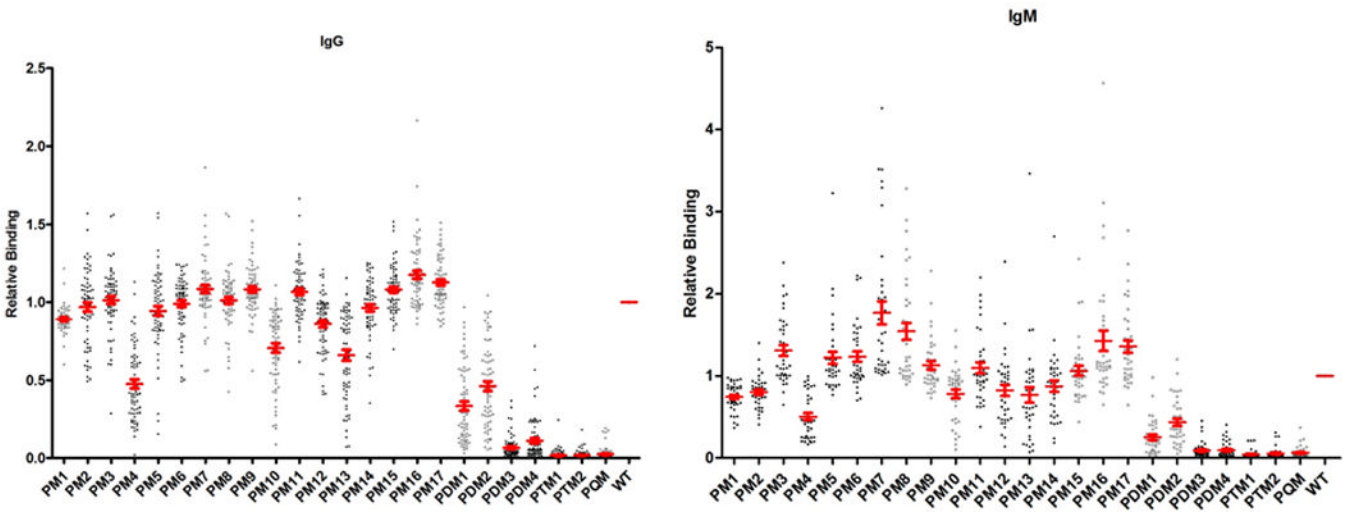

Figure 2.

IgG and IgM relative binding reactivity of PBC sera against wild type PDC-E2 and PDC-E2 mutants. Individual rPDC-E2 mutant proteins were coated onto 96-well ELISA plates and assayed for their reactivity with PBC and non-PBC controls by ELISA. The Y-axis represents the relative Ig reactivities of each mutant normalized to wild type. IgG reactivity of PBC sera to proteins with single alanine substitutions (PM4, PM10, PM13), 4 double alanine substitutions, 2 triple alanine substitutions and one quadruple substitution were significantly reduced IgM reactivity ($P<0.001$). IgM reactivity of PBC sera to proteins with single alanine substitutions (PM4, $P<0.01$), 4 double alanine substitutions, 2 triple alanine substitutions and one quadruple substitution were significantly reduced ($P<0.001$).

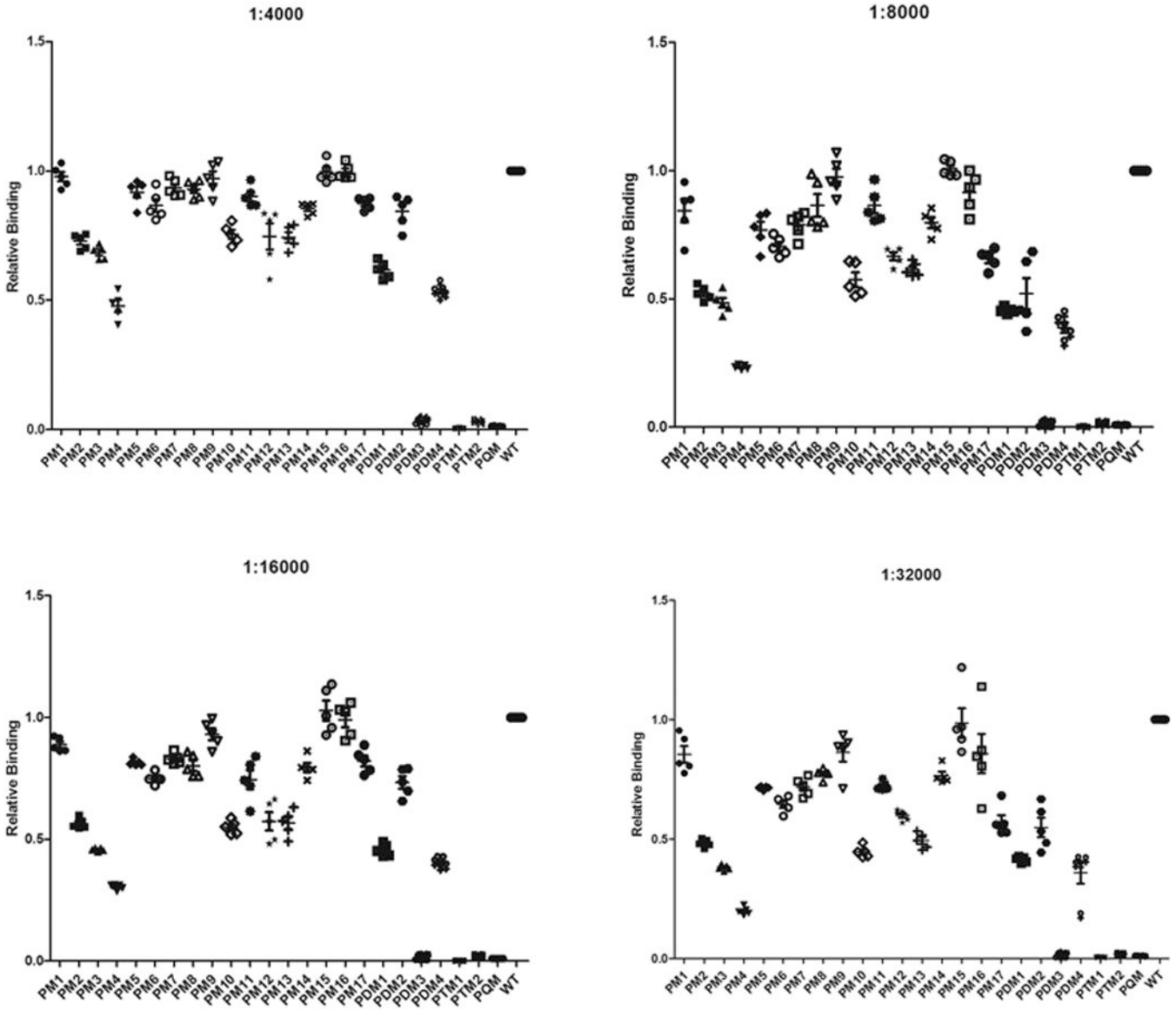

Figure 3.

Determination of intra-assay variability of IgG reactivity to mutant rPDC-E2 and wild type rPDC-E2. rPDC-E2 proteins were coated onto 96-well ELISA plates and assayed for reactivity at serial dilutions and replicated five times. The Y-axis represents relative Ig reactivities of each mutant normalized to wild type.

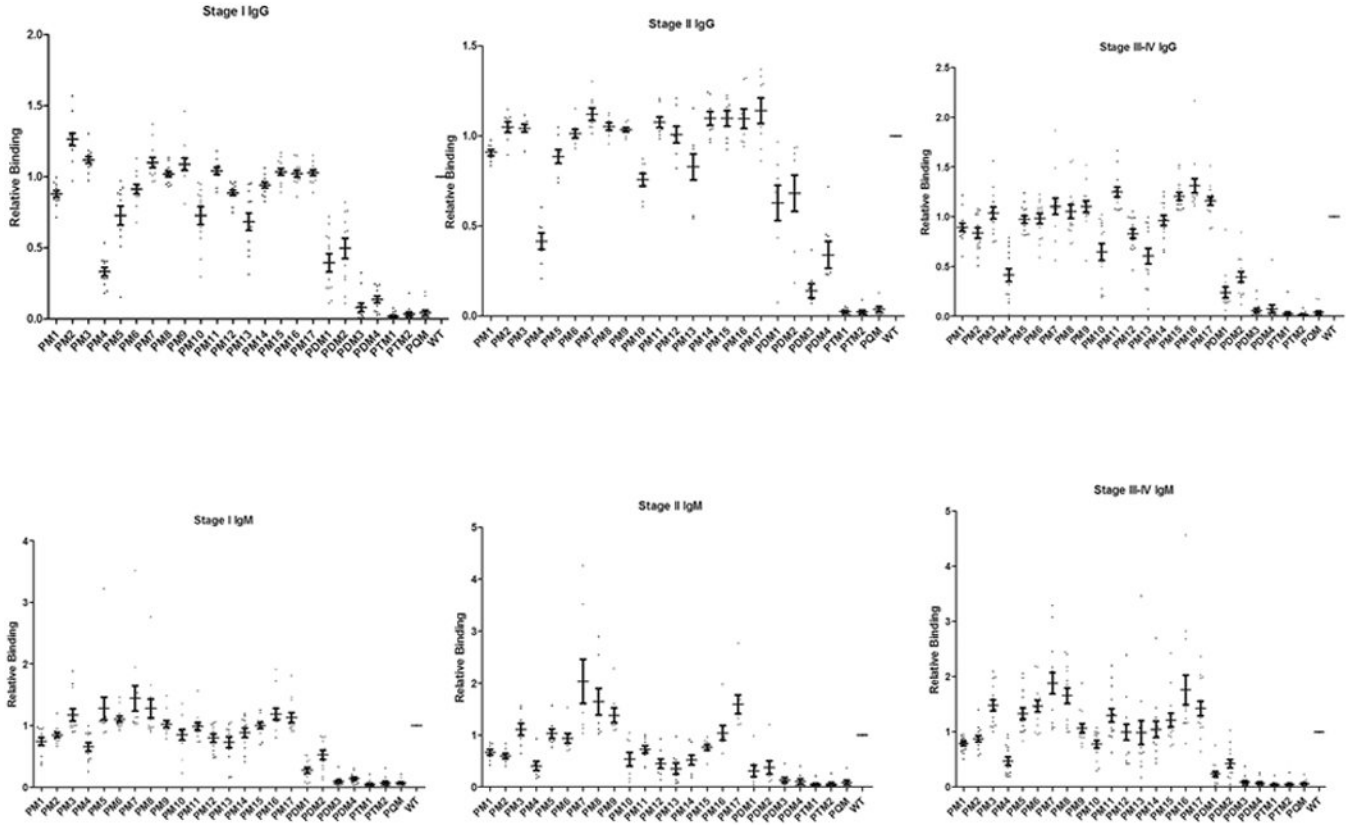

Figure 4.

Relative binding of PBC sera, including patients in stage I (n=20), stage II (n=20) and stage III and IV together (n=20) against PDC-E2 mutants. Individual rPDC-E2 mutant proteins were coated on 96-well ELISA plates and assayed for reactivity with PBC and control sera by ELISA. The Y-axis represents the relative Ig reactivities of each mutant normalized to wild type. Note that reactivity of PBC sera to proteins of mutant #4, including the multiple alanine constructs significantly reduced reactivity ($p<0.001$).

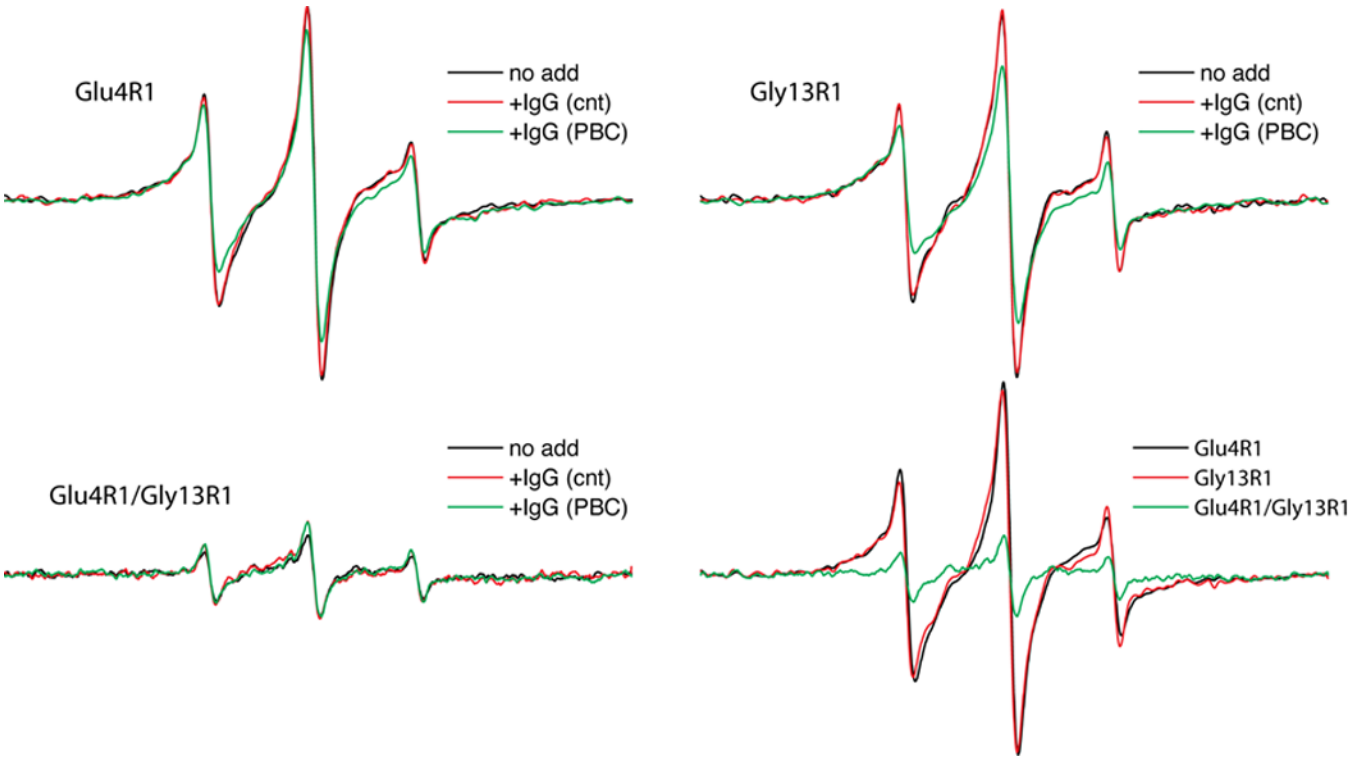

Figure 5.

X-band EPR spectra of rPDC-E2 containing spin labels targeted to the inner lipoyl domain of the PDM3 mutant. Spin label locations are numbered according to the domain positions provided in Table I. The rPDC-E2 concentration in each sample was ~0.5 mg/ml, and all spectral amplitudes are normalized to the same protein concentration. IgG was added to a stiochiometric level with the rPDC-E2 protein.

Table I

Alanine substitution of the PDC-E2 lipoyl domain

Residue Substitution	PDCE2 Mutant	Amino Acid Sequence
		LLAEIETDKATIGFEVQEE
Single Residue Substitution	PLeu1Ala(PM1)	A******************
	PLeu2Ala(PM2)	*A******************
	Wild Type	no change
	PLeu4Ala(PM3)	***A***************
	PIle5Ala(PM4)	****A**************
	PGlu6Ala(PM5)	*****A*************
	PThr7Ala(PM6)	******A************
	PAsp8Ala(PM7)	*******A***********
	PLys9Ala(PM8)	********A**********
	Wild Type	no change
	PThr11Ala(PM9)	**********A********
	PIle12Ala(PM10)	***********A*******
	PGly13Ala(PM11)	************A******
	PPhe14Ala(PM12)	*************A*****
	PGlu15Ala(PM13)	**************A****
	PVal16Ala(PM14)	***************A***
	PGln17Ala(PM15)	****************A**
	PGlu18Ala(PM16)	*****************A*
	PGlu19Ala(PM17)	******************A
Double Residue Substitution	PLeu2Ala/Ile12Ala (PDM1)	*A*********A*******
	PLeu2Ala/Glu15Ala (PDM2)	*A*************A****
	PIle5Ala/Ile12Ala (PDM3)	****A******A*******
	PIle5Ala/ Glu15Ala (PDM4)	****A*********A****
Triple Residue Substitution	PLeu2Ala/Ile5Ala/ Ile12Ala(PTM1)	*A**A******A*******
	PIle5Ala/Ile12Ala/Glu15Ala(PTM2)	****A******A**A****
Quadruple Residue Substitution	PLeu2Ala/Ile5Ala/Ile12Ala/Glu15Ala (PQM)	*A**A******A**A****

Table II

Serological reactivity of PBC to the E2 lipoyl domain mutant constructs.

Mutant No.	PBC Sera[a]		Purified PBC IgG[b]
	IgG	IgM	
WT	1	1	1
PM 1	0.891±0.014	0.741±0.021	0.938±0.084
PM 2	0.968±0.029	0.804±0.032	0.874±0.057
PM 3	1.013±0.025	1.310±0.066	0.807±0.044
PM 4	0.476±0.029***	0.504±0.043**	0.408±0.052***
PM 5	0.944±0.031	1.220±0.073	0.797±0.066
PM 6	0.990±0.022	1.233±0.063	0.888±0.031
PM 7	1.084±0.024	1.768±0.141***	0.848±0.029
PM 8	1.011±0.022	1.542±0.103***	0.876±0.019
PM 9	1.081±0.018	1.129±0.052	1.088±0.030
PM 10	0.706±0.029***	0.781±0.054	0.552±0.065***
PM 11	1.066±0.021	1.096±0.067	0.700±0.065**
PM 12	0.861±0.023	0.823±0.069	0.729±0.055*
PM 13	0.659±0.034***	0.768±0.096	0.482±0.074**
PM 14	0.962±0.022	0.876±0.069	0.848±0.053
PM 15	1.081±0.019	1.062±0.060	0.858±0.045
PM 16	1.175±0.025	1.426±0.124**	1.022±0.039
PM 17	1.126±0.019	1.357±0.076***	0.851±0.088
PDM 1	0.334±0.029***	0.253±0.034***	0.075±0.023***
PDM 2	0.461±0.031***	0.435±0.045***	0.663±0.069***
PDM 3	0.066±0.009***	0.093±0.016***	0.024±0.007***
PDM 4	0.111±0.017***	0.095±0.016***	0.043±0.016***
PTM 1	0.017±0.004***	0.044±0.009***	0.038±0.017***
PTM 2	0.019±0.003***	0.054±0.012***	0.050±0.007***
PQM	0.024±0.005***	0.066±0.012***	0.075±0.031***

[a] Relative ratio of IgG and IgM reactivity to wild type determined by ELISA at 1:4000 sera dilution (n=60).

[b] Relative ratio of purified IgG reactivity to wild type determined by ELISA (n=10).

Asterisks indicate significant differences between mutant protein and wild type protein (*, $p < 0.05$; **, $p < 0.01$; ***, $p < 0.001$; two-tailed unpaired t-test with Welch's correction).

Table III

Comparison of PDC-E2 motifs [a].

Species	Protein	Sequence Motif
Human	PDC-E2	LLAEIETDKATIGFEVQEE
Escherichia coli	PDC-E2	VLVEIETDKVVLEVPASAD
Novosphingobium aromaticivorans	PDC-E2	IMAEIETDKATMEFEAVDE
Chlamydia pneumoniae	PDC-E2	VIVEISTDKAILEHTANED
Lactobacillus delbrueckii	Beta-galactosidase	LVAEKLGPIRSEQLEFTLA

[a]The amino acid residues corresponding to the anchoring isoleucine and glutamic acid at positions 5, 12 and 15 of the human PDC-E2 lipoyl peptide are highlighted.